Supporting information

Optoelectronic performance of perovskites Cs_2KMI_6 (M = Ga, In) based on high-throughput screening and first-principles calculations

Fangfang Qi[a,b,c], Xin Lv[a,c], Jinhui Song[a,c], Xifeng Fu [a, b, c], Lingyi Meng[a,b,c,*,] and Can-Zhong Lu[a,b,c,d,*]

a CAS Key Laboratory of Design and Assembly of Functional Nanostructures, and Fujian Provincial Key Laboratory of Nanomaterials, Fujian Institute of Research on the Structure of Matter, Chinese Academy of Sciences, Fuzhou, Fujian 350002, P. R. China

b College of Chemistry and Materials Science, Fujian Normal University, Fuzhou, Fujian 350007, P. R. China

c Xiamen Key Laboratory of Rare Earth Photoelectric Functional Materials, Xiamen Institute of Rare Earth Materials, Haixi Institutes, Chinese Academy of Sciences, Xiamen 361021, P. R. China

d University of Chinese Academy of Sciences, Beijing 100049, P. R. China

*Corresponding authors.

E-mail address: lymeng@fjirsm.ac.cn (L. Meng) and czlu@fjirsm.ac.cn (C. Lu)

Table S1. Shannon radius of elements in site A, M(I), M(III) and X[1].

Site	Ion type	Radius(Å)	Site	Ion type	Radius(Å)
A	Cs^{+}	1.88	M(III)	Al^{3+}	0.535
	K^{+}	1.64		As^{3+}	0.58
	Na^{+}	1.39		Au^{3+}	0.85
	Rb^{+}	1.72		Bi^{3+}	1.03
M(I)	Ag^{+}	1.15		Ga^{3+}	0.62
	Au^{+}	1.37		In^{3+}	0.80
	Cu^{+}	0.77		Sb^{3+}	0.76
	In^{+}	0.80		Sc^{3+}	0.745
	K^{+}	1.38		Y^{3+}	0.9
	Li^{+}	0.76	X	F^{-}	1.33
	Na^{+}	1.02		Cl^{-}	1.81
	Rb^{+}	1.52		Br^{-}	1.96
	Tl^{+}	1.50		I^{-}	2.2
	Cs^{+}	1.67			

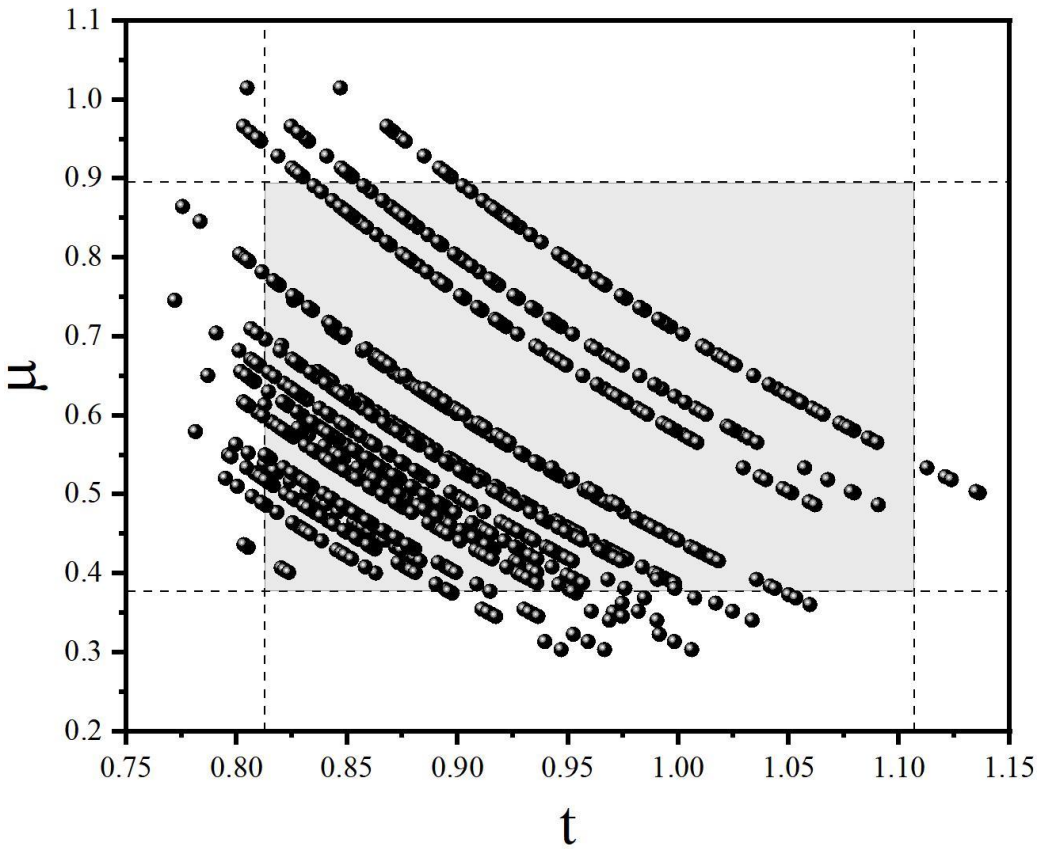

Figure S1. The structural factors of $A_2M(I)M(III)X_6$ compounds.

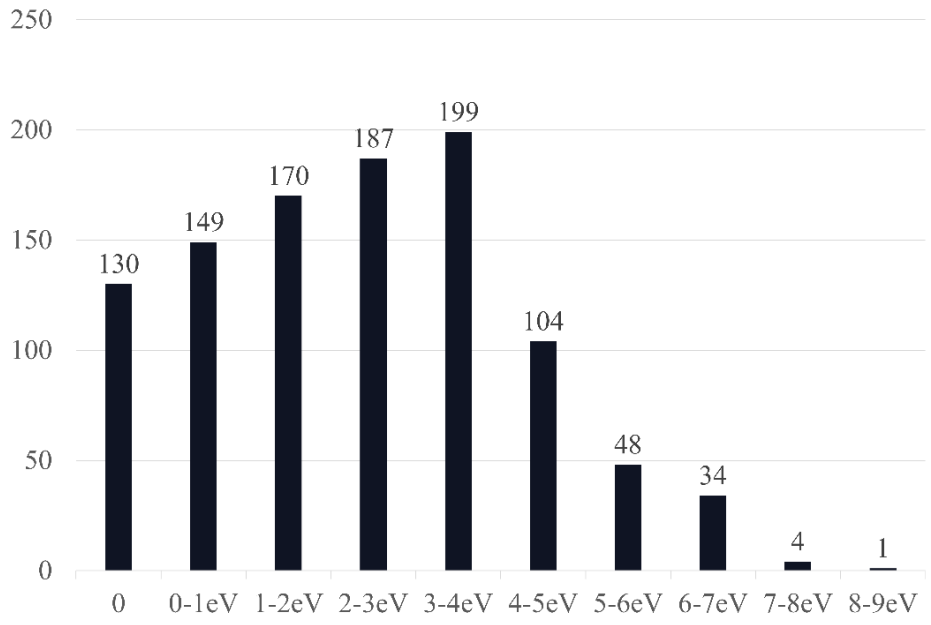

Figure S2. Bandgaps distribution of 1026 $A_2M(I)M(III)X_6$ perovskite compounds derived from the Materials Project database[2].

Table S2. Predicted decomposition energies ΔH_D^P of 23 $A_2M(I)M(III)X_6$ perovskite compounds[3].

Compound	ΔH_D^P **(eV)**	**Compound**	ΔH_D^P **(eV)**
$Cs_2AgAlBr_6$	0.1058	Cs_2TlAsI_6	0.0446
$Cs_2AgGaCl_6$	0.1372	$Cs_2TlSbBr_6$	0.0517
$Cs_2AgInCl_6$	0.1213	$K_2AgGaCl_6$	0.0866
$Cs_2InBiBr_6$	0.0046	$K_2AgInCl_6$	0.0733
$Cs_2InSbCl_6$	0.0043	$K_2AuAlCl_6$	0.1207
Cs_2KGaI_6	0.0307	$K_2InSbCl_6$	-0.0435
Cs_2KInI_6	0.0262	$Rb_2AgGaCl_6$	0.1028
Cs_2KTlBr_6	0.0553	$Rb_2AgInCl_6$	0.0883
$Cs_2LiTlBr_6$	0.0641	$Rb_2AuAlCl_6$	0.1381

$Cs_2NaTlBr_6$	0.0576	$Rb_2InSbCl_6$	-0.0276
Cs_2RbGaI_6	0.0292	$Rb_2TlAsBr_6$	0.0359
$Cs_2TlAsBr_6$	0.0682		

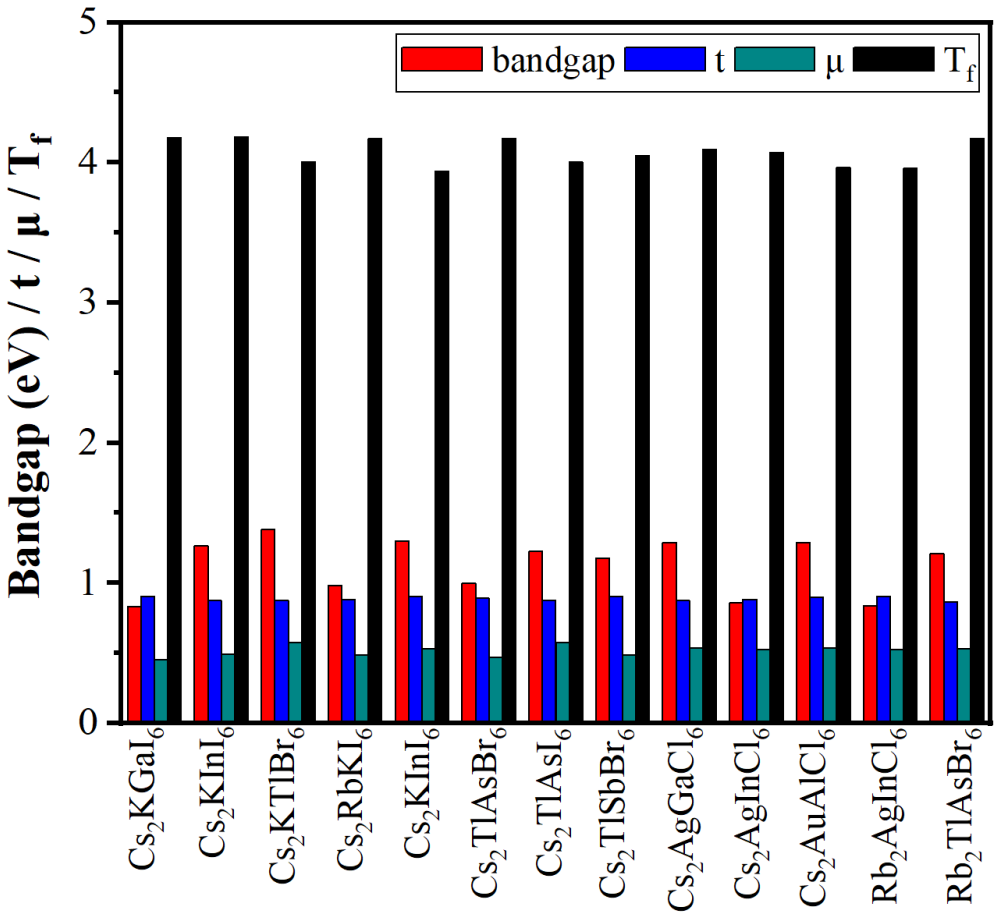

Figure S3. Bandgaps and structural factors of 13 selected $A_2M(I)M(III)X_6$ perovskite compounds, based on the Materials Project database[2].

Table S3. The calculated elastic constants C_{11}, C_{12}, C_{44}, bulk modulus B, shear modulus G, Pugh's ratio (B/G), Poisson's ratio ν[4] of Cs_2KMI_6 (M = Ga, I) based on the PBE functional[5].

	C_{11} (GPa)	C_{12} (GPa)	C_{44} (GPa)	C_{11} - C_{12}	C_{11} + 2C_{12}	B (GPa)	G (GPa)	B/G	*v*
Cs_2KGaI_6	26.39	7.85	7.13	18.54	42.09	14.03	7.99	1.76	0.261
Cs_2KInI_6	26.88	7.18	5.27	19.7	41.24	13.75	7.11	1.93	0.280

Table S4. Calculated formation energies for $Cs_aK_bM_cI_d$ (M = Ga, In) based on the PBE functional[5].

Compound	**Cs_2KGaI_6**	**Cs_2KInI_6**	**CsI**	**KI**	**CsK_2**
$\mathbf{\Delta H_{Cs_aK_bM_cI_d}(eV)}$	-13.54	-13.82	-3.13	-3.00	-3.07
Compound	GaI_3	Ga_2I_3	$CsGa_3$	$CsGa_7$	$KGaI_4$
$\mathbf{\Delta H_{Cs_aK_bM_cI_d}(eV)}$	-2.01	-2.22	-0.67	-1.04	-5.31
Compound	InI	InI_2	InI_3	$CsIn_3$	Cs_2In_3
$\mathbf{\Delta H_{Cs_aK_bM_cI_d}(eV)}$	-0.97	-1.58	-2.03	-0.60	-0.87

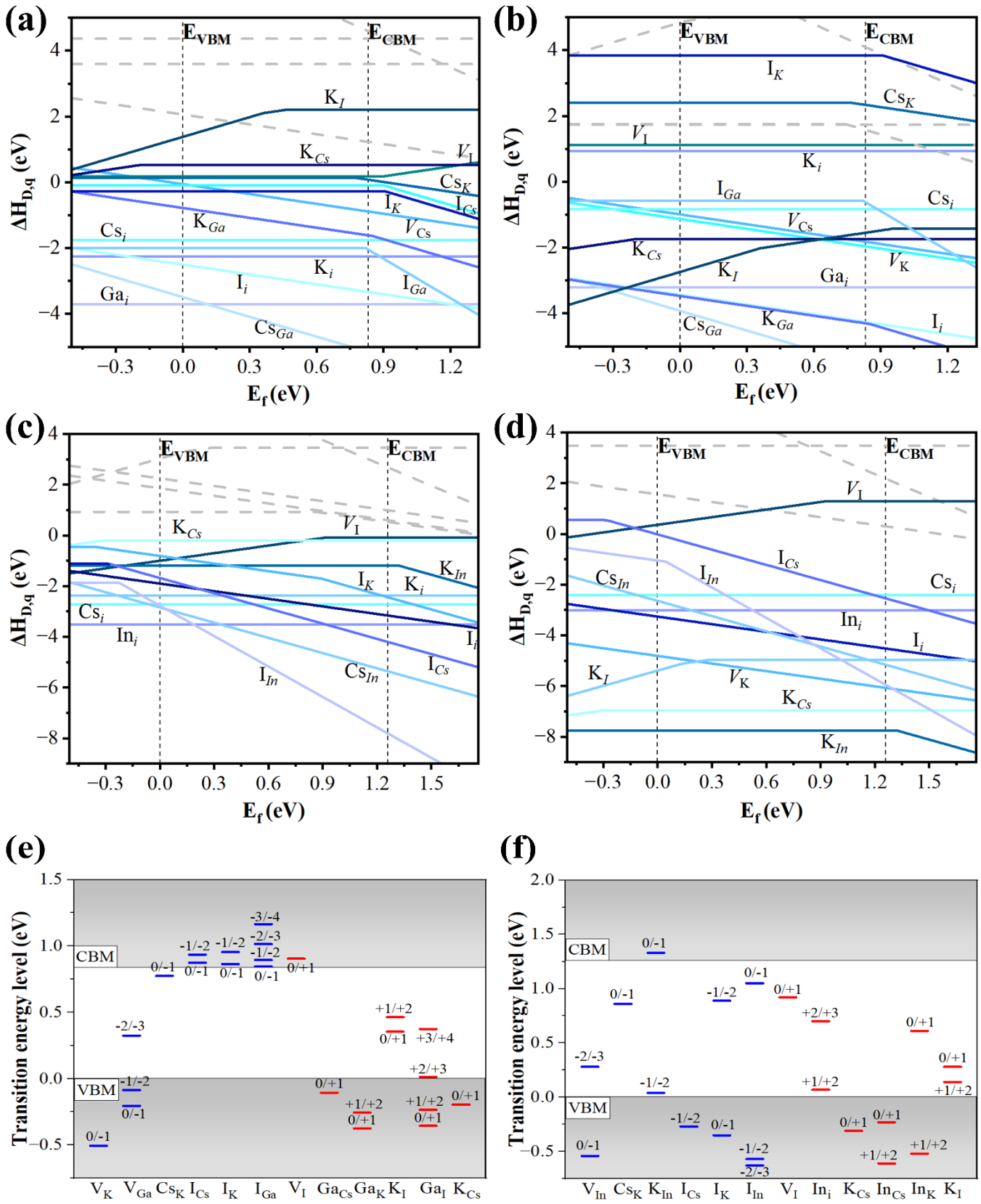

Figure S4. Calculated formation enthalpies $\Delta H_{D,q}$ of intrinsic defects in Cs_2KMI_6 (M = Ga, In) as the function of Fermi level E_f, corresponding the representative chemical potential points in Fig. 2: (a) A (Ga-rich), (b) B (Ga-poor), (c) C (In-rich) and (d) D (In-poor). The solid lines show the trend of formation

enthalpies of the most stable charge states at particular defects change with Fermi level. The grey dashed lines represent the defects with high $\Delta H_{D,q}$s. The slope of the line segment corresponds the charge state q, while the turning points correspond the charge-state transition energy levels. The Fermi level is aligned to the VBM of pristine crystals[6]. Charge-state transition levels of the major intrinsic defects: (e) Cs_2KGaI_6 (f) Cs_2KInI_6.

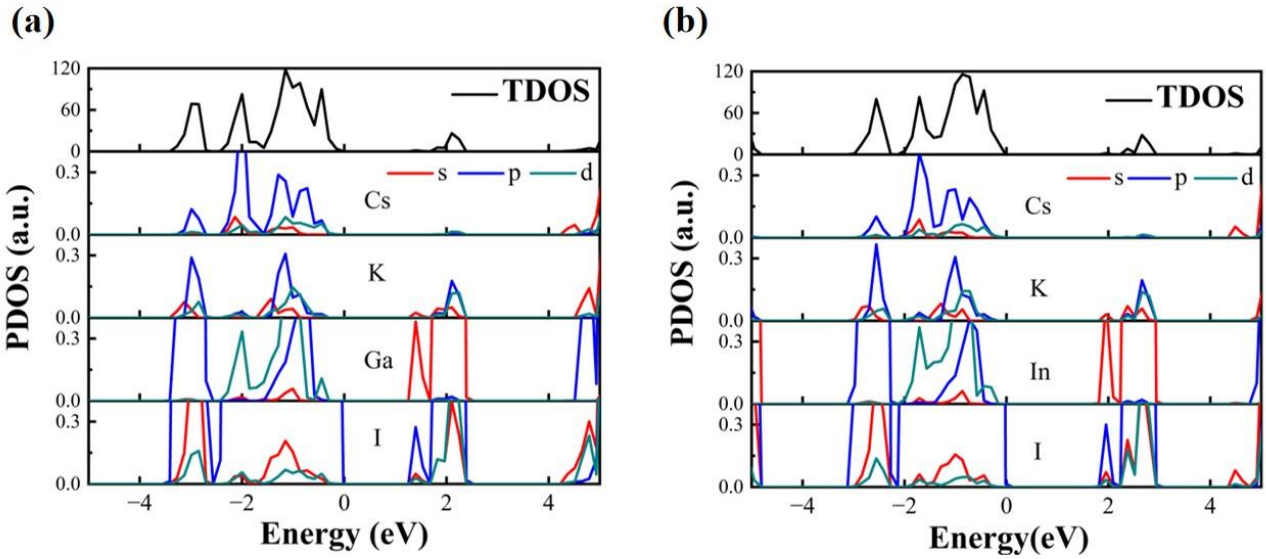

Figure S5. Total and projected density of states (TDOSs and PDOSs) of (a) Cs_2KGaI_6 and (b) Cs_2KInI_6. The calculations are based on the HSE06 functional[7, 8].

REFERENCES

1 R. D. Shannon, *Acta Cryst. A*, 1976, **32**, 751-767.
2 Materials Project database, https://materialsproject.org/.
3 Q. Sun and W. J. Yin, *J. Am. Chem. Soc.*, 2017, **139**, 14905-14908.
4 M. Born, K. Huang and M. Lax, *Am. J. Phys.*, 1955, **23**, 474-474.
5 J. P. Perdew, K. Burke and M. Ernzerhof, *Phys. Rev. Lett.*, 1996, **77**, 3865-3868.
6 J. Xu, J. B. Liu, B. X. Liu and B. Huang, *J. Phys. Chem. Lett.*, 2017, **8**, 4391-4396.
7 J. Heyd, G. E. Scuseria and M. Ernzerhof, *J. Chem. Phys.*, 2004, **118**, 8207-8215.
8 J. Paier, M. Marsman, K. Hummer, G. Kresse, I. C. Gerber and J. G. Angyan, *J. Chem. Phys.*, 2006, **124**, 154709.